Available online at www.sciencedirect.com
ScienceDirect
Journal of Solid State Chemistry 180 (2007) 276–283
JOURNAL OF SOLID STATE CHEMISTRY
www.elsevier.com/locate/jssc

Nanosized aluminum nitride hollow spheres formed through a self-templating solid–gas interface reaction

Jie Zheng[a,*], Xubo Song[a], Yaohua Zhang[a], Yan Li[a], Xingguo Li[a,b], Yikang Pu[c]

[a]*The State Key Laboratory of Rare Earth Materials Chemistry and Applications, College of Chemistry and Molecular Engineering, Peking University, Beijing, 100871, China*
[b]*College of Engineering, Peking University, Beijing, 100871, China*
[c]*Department of Engineering Physics, Tsinghua University, Beijing, China*

Received 31 July 2006; received in revised form 29 September 2006; accepted 16 October 2006
Available online 21 October 2006

Abstract

Nanosized aluminum nitride hollow spheres were synthesized by simply heating aluminum nanoparticles in ammonia at 1000 °C. The as-synthesized sphere shells are polycrystalline with cavity diameters ranging from 15 to 100 nm and shell thickness from 5 to 15 nm. The formation mechanism can be explained by the nanoscale Kirkendall effect, which results from the difference in diffusion rates between aluminum and nitrogen. The Al nanoparticles served as both reactant and templates for the hollow sphere formation. The effects of precursor particle size and temperature were also investigated in terms of product morphology. Room temperature cathode luminescence spectrum of the nanosized hollow spheres showed a broad emission band centered at 415 nm, which is originated from oxygen related luminescence centers. The hollow structure survived a 4-h heat treatment at 1200 °C, exhibiting excellent thermal stability.

Keywords: Aluminum nitride; Hollow spheres; Self-templating; Kirkendall effect

1. Introduction

Materials with hollow structures exhibit distinct physical properties from their solid counterparts and they are advantageous in many application areas such as structural materials [1,2], catalysis [3,4], surface plasmon devices [5,6], gas storage [7], sensors [8] and drug delivery [9]. Controlled synthesis of nanosized hollow spheres has attained much research interest during the last decade. Nanosized hollow spheres of metals [3,10,11], oxides [8,12–14], semiconductors [15–18] and polymers [19–22] have been synthesized. Amongst the various strategies to synthesize hollow spherical structures, utilizing a sacrificed template is the most popular method. To date, a large variety of template materials have been reported including polystyrene beads [21,23], silica spheres [3], carbon spheres [8,15], colloidal metal nanoparticles [10,11], emulsions [19], vesicles [22,24], liquid droplets [5] and even gas bubbles [18]. Materials with layer structure such as BN [25], MoS_2 [26] and $NiCl_2$ [27] spontaneously form hollow structure by bending their layers at suitable conditions. Hollow structures could also be formed by self-assembly or orientation attachment of nanoparticles [12,13,28]. Recently, a method to convert solid nanoparticles into hollow spheres by interface reactions and diffusion based on the nanoscale Kirkendall effect was also developed [29,30].

Gourp III nitrides including AlN, GaN and InN are important semiconductor materials for electronic and optical device applications. AlN is especially attractive for its mechanical hardness, excellent thermal conductivity and endurance to high temperature and chemical corrosion, which make AlN a promising material for harsh environment performance. During the past a few years, AlN nanomaterials with various morphologies have been synthesized, such as nanotubes [31], nanowires [32], nanobelts [33], and nanotips [34,35]. However, the synthesis of nanosized hollow spheres of AlN and other nitrides

*Corresponding author. Fax: +86 10 6276 5930.
E-mail address: xgli@pku.edu.cn (J. Zheng).

0022-4596/$ - see front matter © 2006 Elsevier Inc. All rights reserved.
doi:10.1016/j.jssc.2006.10.011

are still challenging. There are only very few reports on the synthesis of nanosized group III hollow spheres at present [15–17].

We reported here a facile method to produce nanoscale AlN hollow spheres with high yield by heating Al nanoparticles in an ammonia atmosphere, in which the Al nanoparticles served as both precursors and templates. The products were well characterized by X-ray diffraction, high resolution transmission electron microscopy and cathode luminescence (CL) spectroscopy. The influences of precursor particle size and reaction temperature on product morphology were investigated. A mechanism based on the nanoscale Kirkendall effect was proposed to interpret the hollow sphere formation. The nanosized AlN hollow spheres exhibited a blue CL emission and high thermal stability, indicating their potential applications as luminescence materials and high temperature structural materials.

Ma et al. [17] reported the nanosized AlN hollow spheres fabricated in a similar method very recently. The results of the two researches were compared in our manuscript. Most of our results were consistent with that of Ref. [17]. The differences were analyzed and discussed.

2. Experimental section

Aluminum nanoparticles were synthesized by hydrogen plasma metal reaction (HPMR) [36]. An aluminum ingot (purities >99.99%) was melted and evaporated by arc in a 1:1 mixture of argon and hydrogen. The evaporated Al condensed into nanoparticles when leaving the hot plasma area and were transported into a filter for collection by circulate pumping. The arc voltage and current were 25 V and 200 A, respectively. The chamber pressure was kept at 600 Torr. The Al nanoparticles were passivated with a mixture of argon and air to prevent the particles from burning before removing from the collector.

The synthesis of nanosized AlN hollow spheres was carried out in a horizontal quartz tube furnace. About 0.1 g Al nanoparticles were loaded in a ceramic boat which was placed in the center of the tube furnace. The system was first evacuated to 0.6 Pa and then flushed with 99.99% Ar three times to remove oxygen and moisture. The system was then filled with Ar to 1 atm and was heated to 1000 °C at 20 °C min^{-1} under a constant Ar flow of 100 standard cubic centimeters per second (sccm). When the furnace temperature reached 1000 °C, the gas flow was switched to a mixture of 25 sccm Ar and 25 sccm NH_3 (99.99%). The system was maintained in that condition for 3 h before it was allowed to cool down to room temperature in a pure argon flow. The powder in the ceramic boat turned from black to gray. It was collected for further characterization.

The crystal structure and phase purity of the product were characterized by X-ray diffraction (XRD, Rigaku D/max-2000 diffractometer, Cu$K\alpha$). The morphology of the product was observed by a transmission electron microscopy (JEOL-JEM 200CX). The microstructure of the product was studied on a high-resolution transmission electron microscopy (Philips Tecani F30). The specific surface area and pore size distribution were measured with a surface area and pore size analyzer (SA3100) with nitrogen as absorbate. CL spectra were collected on a Monocl cathode luminescence detector (Gatan Co.) equipped on an environmental scanning electron microscope (FEI Quanta 200F) at 15 kV acceleration voltage at room temperature.

3. Results and discussion

Fig. 1a is the XRD pattern of the Al nanoparticles synthesized by HPMR. The diffraction peaks can be indexed as the face centered cubic phase Al (JCPDS 04-0787). Though a protective layer of oxide is supposed to be formed around each particle during the passivation process, no peaks corresponding to oxide or other impurities are detected, suggesting that the oxide phase is probably amorphous. No significant peak broadening is observed. These features indicate that the Al nanoparitcles are of high purity and good crystallinity.

Fig. 2a is a typical TEM image of the Al precursors. The particles are spherical in shape with relatively broad size distribution ranging from 10 to 150 nm. The specific surface area of the Al nanoparticles is 48.3 $m^2 g^{-1}$. Assuming all particles to be identical spheres, the average particle diameter was calculated to be 46 nm, in good agreement with TEM observation.

Fig. 1b and d are the XRD patterns of the products with nitridation duration of 30 min and 3 h, respectively. The diffraction peaks of the fully nitridated product (Fig. 1c) are indexed as the wurtzite aluminum nitride (JCPDS 25-1133). The cell parameters of the AlN nanosized hollow

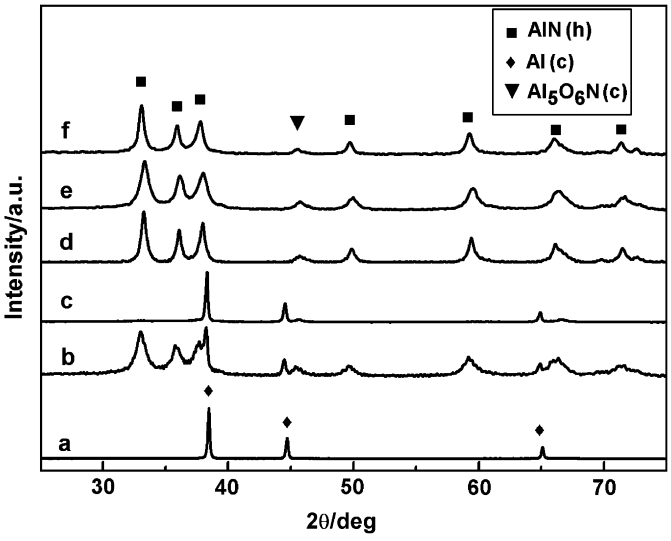

Fig. 1. (a) X-ray diffraction (XRD) pattern of Al nanoparticles synthesized by HPMR. (b)–(f) XRD patterns of Al nanoparticles after heating in 50% NH_3 at different temperature for different time spans: (b) 1000 °C, 30 min; (c) 800 °C, 3 h; (d) 1000 °C, 3 h; (e) 1200 °C, 3 h and (f) 1000 °C, 3 h followed by 1200 °C, 4 h.

spheres were calculated to be $a = 3.108$ Å and $c = 4.974$ Å, slightly smaller than that of the bulk sample. The low peak located at 45.5° indicates the existence of a small amount of crystalline oxide, which best matches the Al_5O_6N phase (JCPDS 48-0686). The oxide phase probably comes from the crystallization of the amorphous surface oxide layers at elevated temperature. The appreciable peak broadening in the XRD pattern of the nitridated products suggests a decrease in grain size after nitridation. Fig. 1b shows the coexistence of diffraction peaks from AlN and Al, indicating incomplete conversion within 30 min.

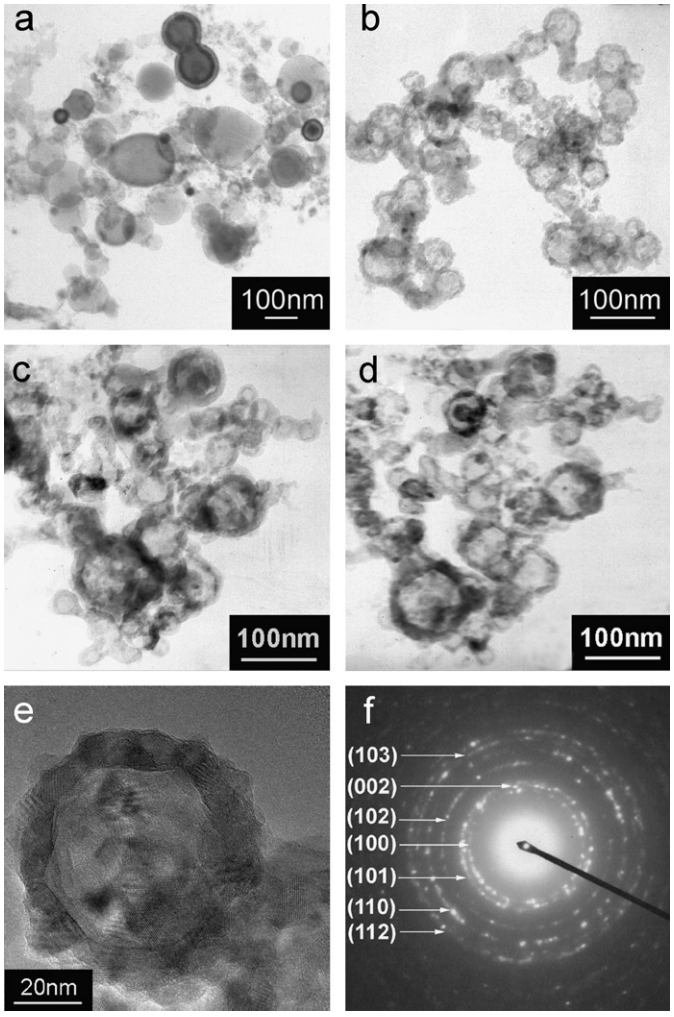

Fig. 2. (a) A transmission electron microscopy (TEM) image of Al nanoparticles synthesized by HPMR. (b, c) Low magnification TEM images of AlN nanosized hollow spheres. (d) The TEM image of the same area as that in (c), but the sample hold was tilted by 20°. (e) A high magnification TEM image of a single AlN nanosized hollow sphere. (f) A typical SAED pattern of an as-synthesized hollow sphere.

Fig. 2b–d are TEM images of the nanosized AlN hollow spheres. The particles exhibited lighter contrast in central parts and darker in peripheries, as shown in Fig. 2b and e. When the TEM sample holder was tilted, the light central areas did not vary, as shown in Fig. 2c and d. These evidences confirm that the obtained products are hollow spheres. The diameters of the hollow cavities range from 15 to 100 nm, comparable to the size of the Al precursors. The typical shell thickness is around 10 nm. From the magnified image of a single hollow sphere (Fig. 2e), the shell is polycrystalline and is composed of densely packed fine nanocrystals. The size of the shell forming nanocrystals is around 10 nm, in consistence with the appreciable broadening peaks in the XRD pattern. The grain boundaries between these particles are rather obscure, indicating their coalescence at high temperature. Fig. 2e is a typical selected area electron diffraction (SAED) pattern of a single hollow sphere. The diffraction rings further confirm that the sphere shell is composed of polycrystalline wurtzite AlN.

Fig. 3a shows the dependence of shell thickness with cavity diameter of the obtained hollow spheres. The shell thickness exhibits an approximately linear increase with the cavity size. The cavity size distribution suggests that the diameter of most hollow spheres (74%) ranges from 10 to 60 nm.

The specific surface area of the hollow spheres was measured to be 36.1 $m^2 g^{-1}$, much less than that of the Al precursors. We expected an increase in specific surface area because both XRD and TEM results indicate appreciable grain size reduction after nitridation, and the formation of hollow spheres creates additional inner surfaces. The paradox can be explained as the aggregation of small nanoparticles. According to our TEM observations, the

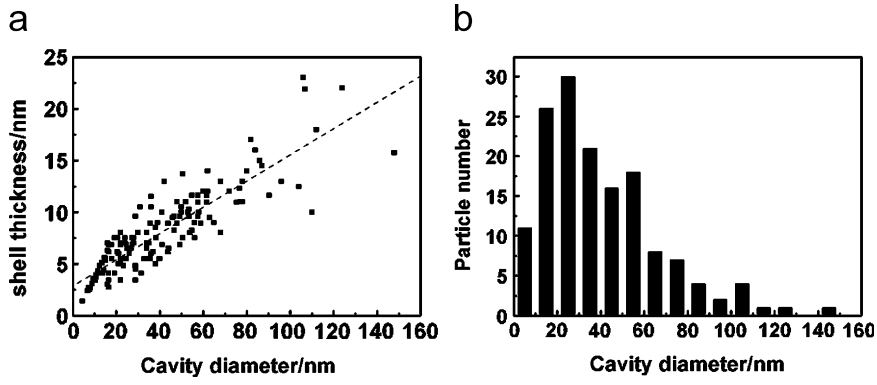

Fig. 3. (a) The dependence of shell thickness with cavity diameters. (b) The cavity diameter distribution of the obtained AlN nanosized hollow spheres. Data was collected from 150 hollow spheres from different TEM images.

shell forming nanocrystals are densely packed. Some smaller hollow spheres also aggregate because of the high reaction temperature. These aggregated particles do not contribute much to the specific surface area even though they are small.

The microstructure of the obtained nanosized hollow spheres was further studied by HRTEM. Fig. 4a is an HRTEM image of the shell. The shell forming nanocrystals exhibit well resolved lattice planes, suggesting the high quality crystallinity of the shell. The distance between adjacent lattice planes is 0.266 nm, consistent with that of the (100) planes of the wurtzite AlN. Energy dispersive X-ray spectra (EDS) were collected at arbitrarily chosen positions of the shell. A typical spectrum is shown in Fig. 4b. Except the main components Al and N, small amount of oxygen is also detected, consistent with the XRD result. The low carbon peak comes from the carbon membrane of the TEM gird. Fig. 4c is the Al concentration profile recorded along the diameter of a nanosized hollow sphere. The apparently lower Al concentration in the central part further confirms the hollow nature of the particle.

Except for some materials with layer structures which are able to form hollow structures spontaneously, templates are usually necessarily employed to obtain hollow structures. In our reaction system, no intentionally template agents were introduced. Considering the comparable size of the aluminum nanoparticle precursors and the obtained AlN hollow nanospheres, it is reasonable to conclude that the aluminum nanoparticles served as both the precursors and templates in the reaction. Similar self-templating effect of metal nanoparticles has already been reported in the formation of other group III nitride hollow spheres [16,17].

The wall thickness of our nanosized hollow spheres increases linearly with the hollow cavity radius, as shown in Fig. 3a. Assuming that the AlN hollow spheres are formed via the Al nanoparticle templates, the linear dependence could be explained. Based on the aluminum mass balance between each spherical shell and the corresponding Al nanoparticle precursor, we have

$$\rho_{\mathrm{AlN}}\left(\frac{4}{3}\pi(r+d)^3-\frac{4}{3}\pi r^3\right)\frac{A_{\mathrm{Al}}}{A_{\mathrm{Al}}+A_{\mathrm{N}}}=\rho_{\mathrm{Al}}\frac{4}{3}\pi r^3,$$

where r is the radius of a precursor Al nanoparticle, d is the shell thickness, ρ_{Al} (or ρ_{AlN}) is the density of Al (or AlN) and A_{Al} (or A_{N}) is the molar mass of Al (or N), respectively. Here, we assume that the cavity is a standard sphere with identical size to that of the corresponding Al precursor. After some simple algebra, we arrive at $d=k(2r)$, where

$$k=\frac{1}{2}\left[\left(\frac{A_{\mathrm{Al}}+A_{\mathrm{N}}}{A_{\mathrm{Al}}}\frac{\rho_{\mathrm{Al}}}{\rho_{\mathrm{AlN}}}+1\right)^{1/3}-1\right]=0.16.$$

The linear regression gives

$$d(\text{in nanometer})=0.13(2r)(\text{in nanometer})+2.9.$$

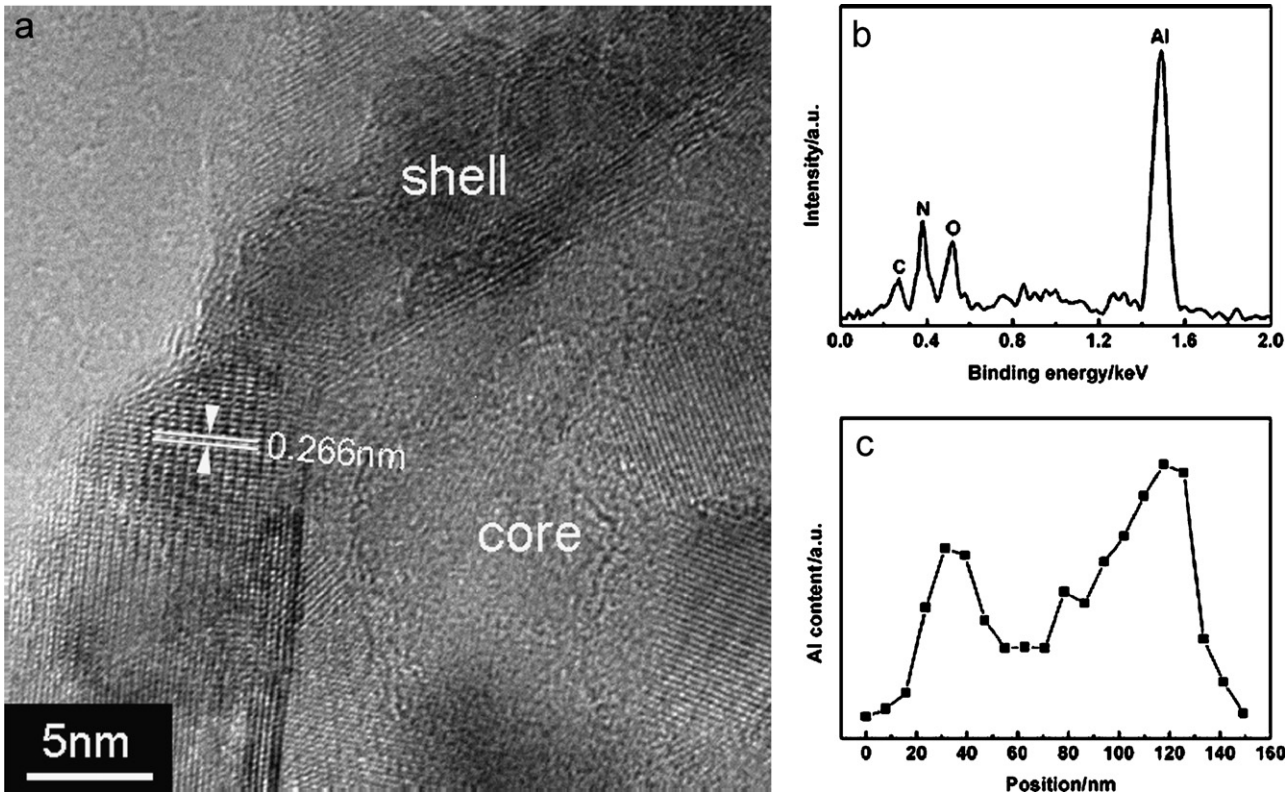

Fig. 4. (a) An HRTEM image of a shell section. (b) The EDS spectrum of an arbitrarily chosen nanosized hollow sphere. (c) The Al content profile along the diameter of an arbitrarily chosen nanosized hollow sphere.

The fairly close results confirm the validity of our simplified model and further support the assumption that the Al nanoparticles served as templates in the reaction.

The self-templating effect of the metal nanoparticles only explains the first step of the nanosized hollow spheres formation. That is, a layer of nitride is formed at the surface of a metal nanparticle. However, it does not tell how the metal core is consumed and why the final product is a hollow sphere instead of a solid particle. When the AlN layer is formed at the surface of each Al nanoparticle through the interface reaction, the Al and N atom have to pass through the AlN layer by solid-state diffusion to meet each other to form AlN. Aluminum was established to be the dominant diffusion species in the Al–N diffusion couple [37]. Therefore, there will be a net outward matter flux and an inward vacancy flux for compensation due to the outward diffusion rate of Al is much faster than the inward diffusion rate of N. The vacancies accumulate at the center of the nanoparticle, leading to the void formation. The vacancy involved diffusion mechanism is known as the Kirkendall effect which was first proposed by E. O. Kirkendall in 1947 [38,39]. This effect has been known to cause void formation for a long time. Its nanoscale effect in leading the formation of nanosized hollow structures was first emphasized by Yin et al. [29] in 2004. In their experiments, cobalt nanoparticles reacted with sulfur contained precursors in the solution. Nanoscale cobalt sulfide hollow spheres were obtained due to the much faster cobalt diffusion rate compared to that of sulfur. This effect is also valid in solid–gas interface reactions. Solid cadmium nanowires could be converted to CdS cylinder shells by a heat treatment in H_2S [30], which was a close analogy to our AlN nanosized hollow sphere formation process. Ma et al. also attributed their AlN hollow sphere formation to this effect [17]. However, due to the difficulty in manipulating the samples with nanoscale size, the intermediate phases of the nanoscale Kirkendall processes are insufficiently investigated at present. More experiment evidence tracing the intermediated phases during the formation process, for example, the in-situ TEM observation is needed to better describe this mechanism. Hollow structures formed through the nanoscale Kirkendall effect usually involve the self-templating effect of one precursor. No additional template agents are needed, which makes this approach an economic way to obtain hollow structures compared to the popular method based on sacrificed templates.

The hollow sphere formation process is illustrated in Fig. 5. First, an AlN layer is formed around the Al droplet through interface reaction (Fig. 5b). Aluminum and nitrogen atoms diffuse across the AlN layer to continue the reaction and thicken the AlN shell. But the outward Al diffusion is much faster, leading to the void formation in the central area (Fig. 5c). The Al core is gradually consumed and a spherical shell is formed (Fig. 5d), with its cavity size close to that of the Al precursor nanoparticle.

Recently, the synthesis of AlN one-dimensional nanomaterials such as nanowires, nanoneedles and nanotubes using conventional chemical vapor deposition technique has been reported. Most of these reactions were carried out around 1000 °C utilizing aluminum and ammonia as reactants [32,34], which were very similar to our experiment condition. However, no vapor transportation phenomenon was observed in our experiment. The distinct

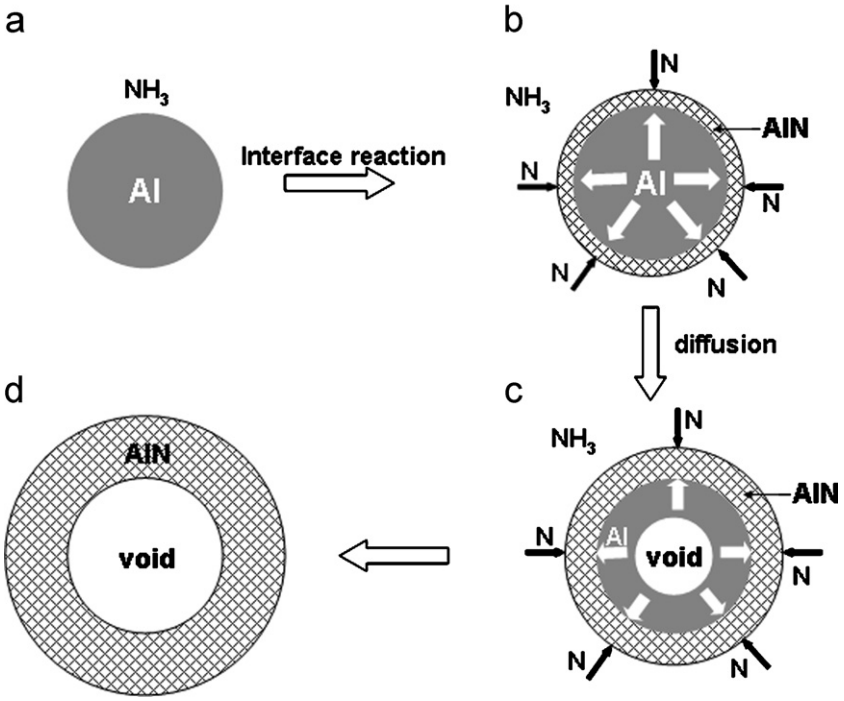

Fig. 5. A schematic illustration of the formation process of nanosized AlN hollow spheres.

behavior could be attributed to the different particle size of the aluminum precursor. Aluminum particles in our experiment are as small as several tens nanometers. The synthesis temperature was high above the melting point of aluminum, at which the aluminum particles were actually liquid droplets. Due to their higher mobility, liquid droplets tend to aggregate to reduce the total surface energy. Their function as templates is no longer valid once aggregation takes place. However, the surface oxide layer of particles could inhibit the aggregation even when the particles are melted. Obviously, the inhibition is more effective for small particles because the effect of grain boundaries and surface species is more prominent for smaller particles. Also, for an oxide layer with a given thickness, smaller liquid droplets are easier to stabilize. Both the above considerations indicate that small size aluminum particles stand a larger chance to maintain their function as templates at the reaction temperature. For comparison, both the aluminum nanoparticles obtained from HPMR and aluminum powder with grain size of several tens μm were heated under a pure argon flow of 50 sccm to 1000 °C and maintained at that temperature for 2 h. After cooling down, the aluminum particles with large grain size aggregated into one integrate metallic ball as expected while the aluminum nanoparticles maintained their dispersive powder form. Therefore, large grain sized aluminum particles are not able to serve as templates for hollow sphere formation because of their aggregation at the reaction temperature. Instead, a conventional chemical vapor transportation and deposition process takes place. The melted aluminum vaporizes, reacts with ammonia in the gas phase, transports to the downstream with carrier gas and deposits as aluminum nitride. In the case of nanosized aluminum particles, the aggregation and the evaporation of aluminum are effectively inhibited by the surface oxide layers. When ammonia is introduced, an interface reaction between Al and NH_3 leads to the formation of AlN nanosized hollow spheres.

Nanosized particles are also more advantageous in the Kirkendall void formation. Hollow structures are able to form only if vacancy accumulation and saturation occur. A directional vacancy flow does not ensure vacancy accumulation since vacancies can be annihilated at dislocations or grain boundaries in bulk materials. While in the case of spherical nanoparticles, the vacancies flow radically to the center of a nanosized sphere and are confined by the nanoscale spherical shells, which facilitates vacancy condensation and hollow structure formation [40].

The influence of the reaction temperature on the product morphology is shown in Fig. 6. When the reaction temperature is 800 °C or lower, nitridation is incomplete (Fig. 1c) and the product morphology does not show significant change to that of the aluminum precursor (Fig. 6a). Temperature higher than 1200 °C leads to the

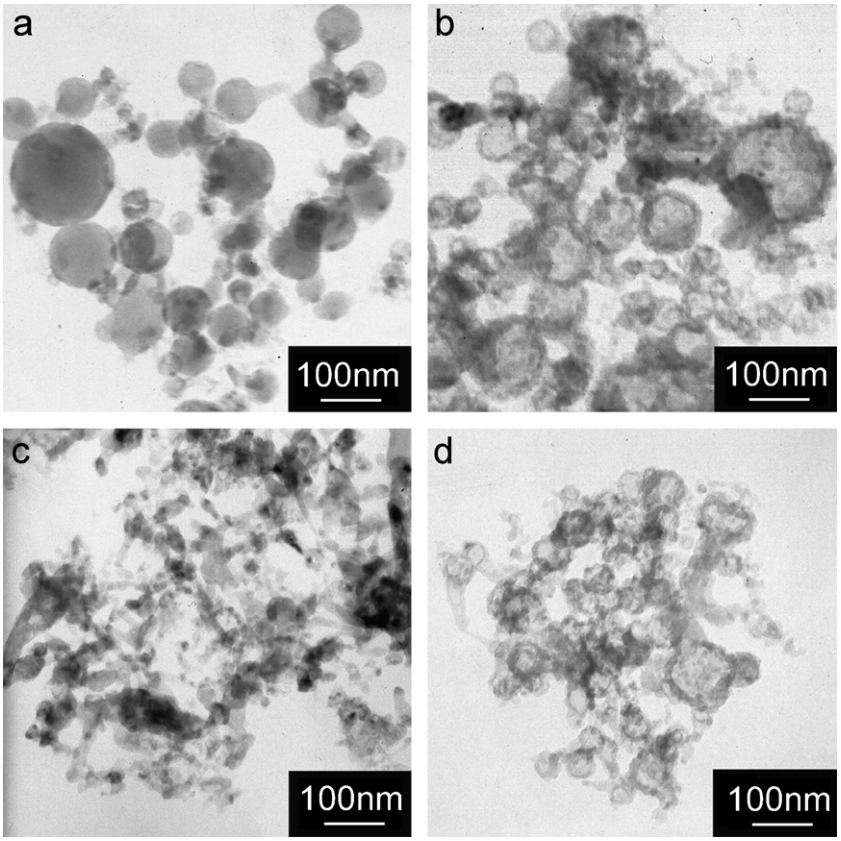

Fig. 6. (a)–(c) TEM images of products obtained under various temperature, (a) 800 °C, (b) 1000 °C, and (c) 1200 °C. (d) A TEM image of hollow spheres after heat treatment in 50% NH_3 atmosphere at 1200 °C for 4 h.

formation of AlN solid particles with elongated shape (Figs. 1e and 6c). The effect of temperature on the product morphology can be understood as the balance of the efficiency of diffusion, which caused hollow structure formation according to the Kirkendall effect, and the maintenance of the separated form of each nanoparticle, which validates them as templates. Lower temperature suppresses diffusion. Although the shape of the precursors is retained, only solid particles are obtained. At higher temperature, the mobility of liquid Al is enhanced, which makes the destruction of template more probable. Even an AlN layer is formed around the Al core, the mobile liquid core makes the infancy of hollow structure fragile. Thus, there exists an optimal temperature which best balances these two facts (Fig. 6b). Similar to the effect of aluminum particle size, the effect of temperature is also related to the stability of templates. In brief, hollow spheres could be formed only if the aluminum templates are stable at temperature allowing effective diffusion to occur. The criterion is of general applicability for hollow structure formation according to the nanoscale Kirkendall effect.

In their recently published work, Ma et al. [17] reported that AlN hollow spheres could be obtained at 1300 °C, which is contradictory to our conclusions. The inconsistence is originated from the difference in the experimental approach. Unlike our procedure in which argon was used, a reactive gas flow was kept through out their heating process. They also raised temperature much slower than we did (3 °C min^{-1}). As a result, it took much longer time when the temperature exceeded 1000 °C in their experiment. Therefore, the AlN hollow spheres were nearly completed when the reaction system entered the high temperature zone. This procedure is equivalent to the formation of AlN hollow spheres at medium temperature (800–1000 °C) followed by the high temperature thermal treatment. The following reaction at high temperature only improved the purity and crystallinity of the hollow spheres but did not destroy their hollow structure. To verify this assertion, we raised the temperature to 1200 °C and kept there for 4 h after the 3 h reaction at 1000 °C under the same gas flow. The structure and morphology of the product show no significant change, as indicated by the XRD pattern (Fig. 1f) and the TEM image (Fig. 6d). We could also conclude that the hollow structures are very stable at high temperature once they are completely formed. The AlN nanosized hollow spheres will be promising high temperature structural materials for their chemical stability, endurance to high temperature and lower density if their mechanical strength can be further testified.

The room temperature CL spectrum of our nanosized hollow spheres shows a broad peak centered at 415 nm (Fig. 7). The optical emission of AlN nanomaterials reported in literatures exhibited similar board emission bands, with maxima ranging from 400 to 500 nm [17,35,41], originated from different trap-level states related to defects or impurities. The emission band around 415 nm was

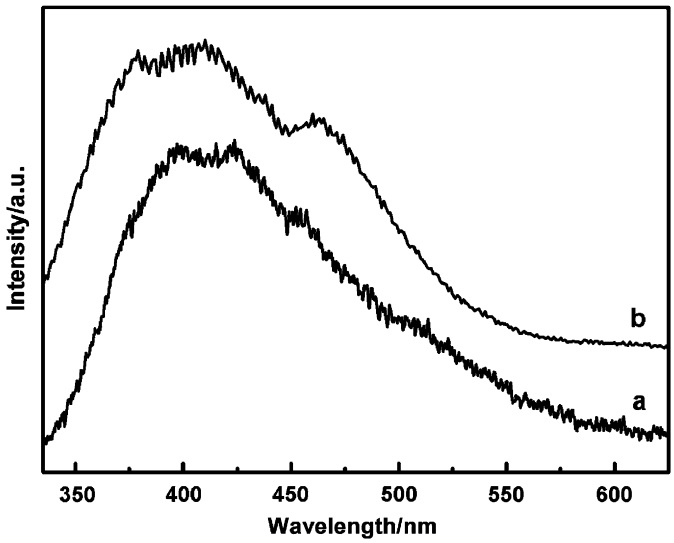

Fig. 7. The cathode luminescence (CL) spectra of (a) the obtained AlN nanosized hollow spheres and (b) AlN solid particles. The solid AlN nanoparticles were synthesized in the same way except that the reaction temperature was set to 1200 °C. The corresponding TEM image was shown in Fig. 6c.

reported to be from oxygen impurity related luminescence centers. The donor was assumed to be an electron trapped on an oxygen impurity (O_N^-), which substitutes for a nitrogen atom on a regular lattice site. The defect structure of the acceptor was established to be a hole trapped on an O_N–V_{Al} complex [42]. Our nanosized AlN hollow spheres contain a detectable amount of oxygen as indicated by XRD and EDS. Therefore, the 415 nm emission of our nanosized hollow spheres is very likely to be from oxygen related luminescence centers, similar to that reported by Schweizer et al. [42] and Trinkler et al. [43]. Compared to the CL spectrum of solid AlN nanoparticles, the shoulder at around 470 nm originated from nitrogen vacancies [35] becomes less prominent in the spectrum of AlN nanosized hollow spheres, indicating that the oxygen related emission is the dominant mechanism for CL of our nanosized AlN hollow spheres.

4. Conclusion

Nanosized AlN hollow spheres with cavity diameter from 15 to 100 nm and wall thickness from 5 to 15 nm were produced by a simple heat treatment of aluminum nanoparticles in ammonia. The sphere shells of the obtained hollow spheres are polycrystalline and are composed of closely packed AlN nanocrystals with wurtzite structure. The hollow structure formation mechanism can be explained by the nanoscale Kirkendall effect in which aluminum nanoparticles served as both reactants and templates. The formation of hollow spheres requires that the aluminum templates are stable at temperature allowing effective diffusion to occur. Thus, nanosized aluminum precursors and a reaction temperature around 1000 °C are necessary. The AlN hollow spheres

have a CL emission band centered at 415 nm at room temperature originated from oxygen related luminescence centers. The hollow structures exhibit high thermal stability and may find applications as potential high temperature structural materials.

Acknowledgments

This work was supported by NSFC (Nos. 20221101 and 10335040) and MOST of China (No. 2001CB610509).

References

[1] J.K. Cochran, Curr. Opin. Solid. State Mater. 3 (1998) 474.
[2] O. Andersen, U. Waag, L. Schneider, G. Stephani, B. Kieback, Adv. Eng. Mater. 2 (2000) 192.
[3] S.W. Kim, M. Kim, W.Y. Lee, T. Hyeon, J. Am. Chem. Soc. 124 (2002) 7642.
[4] H.P. Liang, H.M. Zhang, J.S. Hu, Y.G. Guo, L.J. Wan, C.L. Bai, Angew. Chem. Int. Ed. 43 (2004) 1540.
[5] H.P. Liang, L.J. Wan, C.L. Bai, L. Jiang, J. Phys. Chem. B 109 (2005) 7795.
[6] S.J. Oldenburg, G.D. Hale, J.B. Jackson, N.J. Halas, Appl. Phys. Lett. 75 (1999) 1063.
[7] T. Miyao, K. Minoshima, S. Naito, J. Mater. Chem. 15 (2005) 2268.
[8] X.L. Li, T.J. Lou, X.M. Sun, Y.D. Li, Inorg. Chem. 43 (2004) 5442.
[9] E. Mathiowitz, J.S. Jacob, Y.S. Jong, G.P. Carino, D.E. Chickering, P. Chaturvedi, C.A. Santos, K. Vijayaraghavan, S. Montgomery, M. Bassett, C. Morrell, Nature 386 (1997) 410.
[10] Y.G. Sun, B. Mayers, Y.N. Xia, Adv. Mater. 15 (2003) 641.
[11] Y.G. Sun, Y.N. Xia, Science 298 (2002) 2176.
[12] A.M. Cao, J.S. Hu, H.P. Liang, L.J. Wan, Angew. Chem. Int. Ed. 44 (2005) 4391.
[13] H.G. Yang, H.C. Zeng, Angew. Chem. Int. Ed. 43 (2004) 5930.
[14] Z.Y. Jiang, Z.X. Xie, X.H. Zhang, S.C. Lin, T. Xu, S.Y. Xie, R.B. Huang, L.S. Zheng, Adv. Mater. 16 (2004) 904.
[15] X.M. Sun, Y.D. Li, Angew. Chem. Int. Ed. 43 (2004) 3827.
[16] L.W. Yin, Y. Bando, M.S. Li, D. Golberg, Small 1 (2005) 1094.
[17] Y.W. Ma, K.F. Huo, Q. Wu, Y.N. Lu, Y.M. Hu, Z. Hu, Y. Chen, J. Mater. Chem. 16 (2006) 2834.
[18] Q. Peng, Y.J. Dong, Y.D. Li, Angew. Chem. Int. Ed. 42 (2003) 3027.
[19] O.D. Velev, K. Furusawa, K. Nagayama, Langmuir 12 (1996) 2374.
[20] F. Caruso, Chem. Eur. J. 6 (2000) 413.
[21] F. Caruso, R.A. Caruso, H. Mohwald, Science 282 (1998) 1111.
[22] J. Hotz, W. Meier, Langmuir 14 (1998) 1031.
[23] Z.Y. Zhong, Y.D. Yin, B. Gates, Y.N. Xia, Adv. Mater. 12 (2000) 206.
[24] H.T. Schmidt, A.E. Ostafin, Adv. Mater. 14 (2002) 532.
[25] N.G. Chopra, R.J. Luyken, K. Cherrey, V.H. Crespi, M.L. Cohen, S.G. Louie, A. Zettl, Science 269 (1995) 966.
[26] J. Etzkorn, H.A. Therese, F. Rocker, N. Zink, U. Kolb, W. Tremel, Adv. Mater. 17 (2005) 2372.
[27] Y.R. Hacohen, E. Grunbaum, R. Tenne, J. Sloan, J.L. Hutchison, Nature 395 (1998) 336.
[28] H.L. Cao, X.F. Qian, C. Wang, X.D. Ma, J. Yin, Z.K. Zhu, J. Am. Chem. Soc. 127 (2005) 16024.
[29] Y.D. Yin, R.M. Rioux, C.K. Erdonmez, S. Hughes, G.A. Somorjai, A.P. Alivisatos, Science 304 (2004) 711.
[30] Q.G. Li, R.M. Penner, Nano Lett. 5 (2005) 1720.
[31] Q. Wu, Z. Hu, X.Z. Wang, Y.N. Lu, X. Chen, H. Xu, Y. Chen, J. Am. Chem. Soc. 125 (2003) 10176.
[32] Y.J. Zhang, J. Liu, R.R. He, Q. Zhang, X.Z. Zhang, J. Zhu, Chem. Mater. 13 (2001) 3899.
[33] Q. Wu, Z. Hu, X.Z. Wang, Y. Chen, Y.N. Lu, J. Phys. Chem. B 107 (2003) 9726.
[34] S.C. Shi, C.F. Chen, S. Chattopadhyay, Z.H. Lan, K.H. Chen, L.C. Chen, Adv. Funct. Mater. 15 (2005) 781.
[35] C. Liu, Z. Hu, Q. Wu, X.Z. Wang, Y. Chen, H. Sang, J.M. Zhu, S.Z. Deng, N.S. Xu, J. Am. Chem. Soc. 127 (2005) 1318.
[36] H.Y. Shao, T. Liu, X.G. Li, Nanotechnology 14 (2003) L1.
[37] T. Telbizova, S. Parascandola, U. Kreissig, R. Gunzel, W. Moller, Appl. Phys. Lett. 76 (2000) 1404.
[38] H. Nakajima, JOM 49 (1997) 15.
[39] A.D. Smigelskas, E.O. Kirkendall, Trans. AIME 171 (1947) 130.
[40] K.N. Tu, U. Gosele, Appl. Phys. Lett. 86 (2005) 093111.
[41] Q. Zhao, H.Z. Zhang, X.Y. Xu, Z. Wang, J. Xu, D.P. Yu, G.H. Li, F.H. Su, Appl. Phys. Lett. 86 (2005).
[42] S. Schweizer, U. Rogulis, J.M. Spaeth, L. Trinkler, B. Berzina, Phys. Stat. Sol. B 219 (2000) 171.
[43] L. Trinkler, B. Berzina, S.C. Shi, L.C. Chen, M. Benabdesselam, P. Iacconi, Phys. Stat. Sol. C 2 (2005) 334.